Investigation of optimization techniques on structural-acoustical shaped concrete slabs in buildings

Jonathan Michael Broyles, Micah R. Shepherd and Nathan C. Brown

Citation: Proc. Mtgs. Acoust. **42**, 022001 (2020); doi: 10.1121/2.0001354

View online: https://doi.org/10.1121/2.0001354

View Table of Contents: https://asa.scitation.org/toc/pma/42/1

Published by the Acoustical Society of America

Volume 42 http://acousticalsociety.org/

179th Meeting of the Acoustical Society of America

Acoustics Virtually Everywhere

7-11 December 2020

*Computational Acoustics: Paper 3pCA2

Investigation of optimization techniques on structural-acoustical shaped concrete slabs in buildings

Jonathan Michael Broyles
Department of Architectural Engineering, The Pennsylvania State University, State College, PA, 16803; jmb1134@psu.edu

Micah R. Shepherd
Department of Acoustics, The Pennsylvania State University, University Park, PA, 16802; mrs30@psu.edu

Nathan C. Brown
Department of Architectural Engineering, The Pennsylvania State University, University Park, PA, 16802; ncb5048@psu.edu

Computational tools have become integrated into design practice at the building scale and component scale. While there has been a resurgence of optimization techniques in room acoustics, research has been limited on utilizing optimization techniques on building components, such as a building's structural floor. Quality design solutions must be found at the component scale to accommodate for increased urbanization, environmental concerns, building utilization, and the well-being of the occupants, especially in relation to the tenants' acoustic environment. This presentation will discuss the use of several design space exploration and optimization approaches to generate and consider multiple permutations of shaped concrete floor designs. The shape of the ribbed slab will be varied in order to improve both the embodied energy of the concrete slab, which is proportional to mass, as well as the sound transmission class (STC). Three computational techniques (Latin Hypercube Sampling, multi-objective evolutionary optimization and constrained optimization) will be used to determine trade-offs in the design. The advantages and disadvantages of each technique will be highlighted with respect to the trade-off between reduced mass and improved STC. Finally, the importance of model resolution will be discussed in early design space exploration and optimization procedures.

Technical Committee on Computational Acoustics Early Career Presenter Award

Published by the Acoustical Society of America

 https://doi.org/10.1121/2.0001354

1. INTRODUCTION

Optimization algorithms and tools have become increasingly integrated into several disciplines in building design practice, from the full building scale down to the component scale. The acoustic performance of a room has recently been considered through design optimization, yet the scope of this research has been limited to large rooms, such as auditoria, and focused on characteristics such as reflection and diffusion [1]. Building design with acoustic optimization at the component scale could provide quality solutions to accommodate for increased urbanization, environmental concerns, building utilization, and the well-being of the occupants, especially in relation to the tenants' acoustic environment [2-4].

This paper discusses the use of several design space exploration and optimization approaches to generate and consider multiple permutations of shaped structural-acoustic concrete floors. The shape of the ribbed slab will be varied to improve both the embodied carbon of the concrete slab, which is proportional to its mass as denoted by its surface density in kg/m^2, as well as the acoustic metric of sound transmission class (STC). Three computational techniques, Latin Hypercube Sampling, Multi-Objective evolutionary Optimization, and Constrained Optimization will be used to determine structural-acoustic design trade-offs. The advantages and disadvantages of each technique will be highlighted with respect to the trade-off between reduced mass and improved STC. Finally, the importance of design space exploration technique resolution will be discussed in early design space exploration and optimization procedures. The goals are to demonstrate how acoustic simulations can be integrated into early stage optimization of building components, and to better understand the pros and cons of various optimization techniques in a multi-disciplinary design process.

2. BACKGROUND

Aside from auditoria, acoustic performance in a building is often neglected in the early phase of design. However, research has shown that acoustic objectives such as sound absorption, sound reflection, and sound transmission in a building can be negatively impacted by primary building design considerations including the structural system, building operations, and lighting. As discussed by Badino *et al.*, acoustic performance is directly linked to architectural design because the room geometry impacts sound behavior; specifically, how the sound is reflected, diffused, or absorbed in the space [1]. Because acoustic performance is linked to architectural design, there are geometric-room acoustic design trade-offs. Including acoustic performance in the early design phase can account for such trade-offs.

As design tools have increasingly improved, the incorporation of acoustics in the early stage of building design has increased. As a result of improved collaboration between acousticians and architects, elaborate geometric and architectural layouts of auditoria were created that provided excellent acoustic environments and distinctive viewpoints of performances such as the novel Philharmonie de Paris [1]. Including acoustic performance in building design is not limited to auditoria, however, as acousticians are often cited for providing acoustic solutions to offices and residential complexes [5]. Acoustical solutions are often necessary in office and residential building design but are commonly implemented post-construction to mitigate existing building acoustic problems. Therefore, the incorporation of acoustic-based performance early in the design phase would address mitigations efforts often incorporated post-construction, proving more valuable to both building owners and tenants.

Acoustic performance-based design has largely been incorporated at a room scale and not at a building element scale. Aside from Méndez Echenagucia *et al.* who evaluated curved structural panels for sound reflection [6] and Roozen *et al.* who investigated airborne sound of funicular shells [7], there is a lack of breadth in this field of research. Consideration of acoustic performance at the building element scale could improve the indoor acoustic environment and resolve acoustic problems post-construction. Acoustic performance-based design has not thoroughly investigated the impact of sound transmission between rooms, likely due to acoustic performance-based design optimization only being incorporated for individual large rooms. Yet research on the incorporation of sound transmission at a building element scale could have significant impacts on the building's utilization, building's cost, and tenant's health and satisfaction in the building.

Despite the void in acoustic performance-based design for sound transmission with the application towards building design, there has been research in sound transmission with a focus in mechanical and aerospace engineering. Furthermore, this research has primarily focused on how a structural system vibrates at certain structural modes under certain boundary conditions. Structural vibrations have been an important topic to many engineering applications including automobiles and airplanes [8]. Traditionally, research on structural-acoustic interaction has involved computational methods such as finite element analysis and boundary element analysis to determine how structural vibration radiates into a surrounding medium [9]. The effect of structural stiffeners on radiated power was thoroughly researched in several curved geometries such as shells [10] and flat panels [11] in addition to sandwich structures [12]. Further, research suggests that the structure's geometry can significantly contribute to acoustic characters including transmission loss [13,14]. Research regarding slight geometric changes with a structural panel suggests that sound transmission could be affected by adjusting the structural geometry for complex floor systems. To investigate how sound transmission and shaped concrete slabs could interact, a method to consider design objectives for both structure and sound simultaneously is needed.

In this research, multiple design space exploration techniques of varying resolutions are utilized. As stated by Touloupaki and Theodosiou, optimization is an iterative process involving the selection of variables and objectives for optimization, the model necessary for simulation, appropriate selection of objectives and optimization techniques, running the simulation until convergence is reached, and data analysis of the results obtained [15]. To evaluate the structural-acoustic trade-offs in the design space of shaped concrete slabs, three computational techniques are used that increase in specificity of desired design performance. These techniques are Latin Hypercube Sampling, Multi-Objective Optimization, and Constrained Optimization. In sampling of the design space, many designs are iterated until the user-inputted design target number is reached. Latin Hypercube Sampling (LHS) is a near-random sampling of the design space that enables a complete sampling of the entire design space, fully exploring the bounds of each defined variable [16]. Multi-Objective Optimization (MOO) is a common optimization technique utilized when evaluating designs based on two or more competing objectives. MOO is performed using the evolutionary, genetic algorithm Non-dominated Sorting Genetic Algorithm-II (NSGA-II) to identify the non-dominated designs for a set of objectives [17]. A non-dominated design is one in which one objective value can't improve without the reduction of a secondary objective value. NSGA-II generates a Pareto curve which enables the designer to identify recurring distributional patterns while exploring observed assignments in the objective space without formal constraints [18,19]. A Pareto curve provides the trade-off of potential solutions based on the objective functions provided in the optimization. A third computational method is Constrained Optimization, which investigates the design space for the best designs when optimizing a single objective. Constrained Optimization converges on the best designs with specified constraints and is performed using the gradient-free algorithm Constrained Optimization By Linear Approximation (COBYLA) [20]. This computational technique is implemented for the multi-objective problem by running a series of optimizations in which one objective performance level is specified as a constraint. Constrained optimization is thus beneficial when a specific value is desired for one objective while optimizing a secondary objective.

The three computational techniques provide different insights into design trade-offs that could not be identified using a single technique. As previously mentioned, research on the acoustic analysis at the component level in building design is also largely unexplored. In response, this paper addresses the following questions: (1) Can a simplified acoustic analysis be implemented in component design to provide information prior to construction? (2) How do design space exploration techniques compare, and how do their practical advantages and disadvantages affect the design outcomes they generate? The research method is explained next, describing the different floor slab geometries, followed by the results and discussion of the study, final conclusions, and future work.

3. METHODS

This section briefly discusses the overall methodology for the multi-disciplinary research as shown in Figure 1. A parametric model was created to permute distinctive shaped concrete slab designs. Parametric modelling incorporated a collection of nine geometric variables with specified bounds that are modulated to generate 3-dimensional models of concrete slabs. Advances in design tools have enabled quick geometric modifications while simultaneously conducting simulations to evaluate the performance implications of these geometric changes. These simulations are used within optimization algorithms to drive the slab geometry towards two objectives: minimizing structural mass, which is expressed by surface density, and related to cost and environmental performance, and maximizing Sound Transmission Class (STC), as described in Eq. 1. The parametric framework is beneficial in the investigation of sustainable design solutions as the concrete slab geometry can be quickly manipulated to reduce the mass by placing the structural material where it is necessary.

$$optimize\ f(x) = \{min(structural\ mass), max\ (STC)\} \quad (1)$$

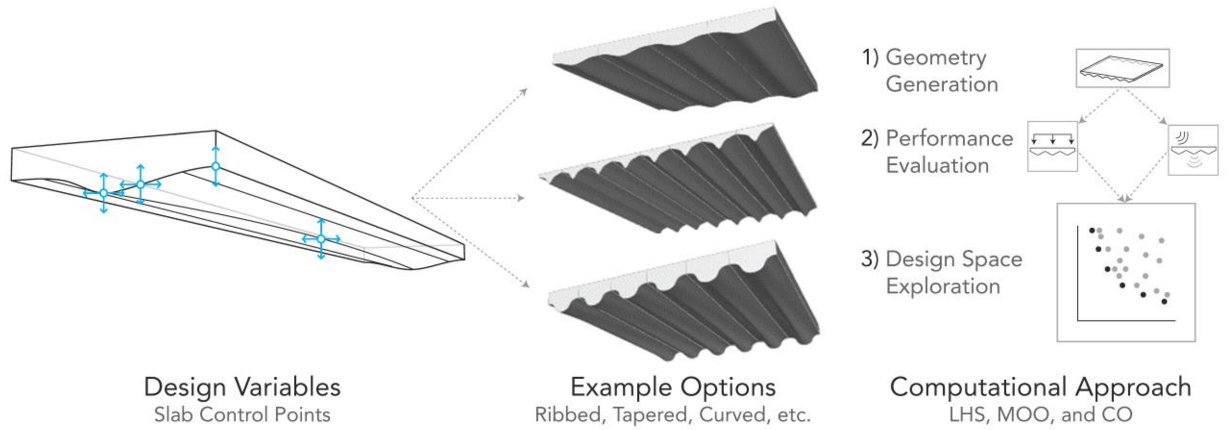

Figure 1. General research method.

A. PARAMETRIC MODEL

With a primary objective of reducing the structural mass, the geometric variables were selected that would provide the highest potential for more flexible and continuous exploration of form, performance, and aesthetics. The nine geometric variables used in the parametric model are: the number of ribs, top slab thickness, rib thickness on the ends, rib thickness in the middle, two curvature points – each with an end width and a taper, and change of the rib's mid-width. Seven of the geometric variables were used to shape a cross section of the shaped slab including both the top slab and the rib. The cross section of the rib was shaped based on the taper and end width of two control points. The depth of the cross section was controlled by the rib depth variable. Although rectilinear shaped slabs can be less laborious than curved shaped slabs, curved slabs have the potential for even less structural material than rectilinear slabs. Curved ribs have not traditionally been researched for their structural-acoustic performance and could provide better objective performance in addition to better secondary objective performance such as aesthetics. With advances in digital fabrication, curvature in concrete has the potential to be competitive with traditional systems if performance improvements and achievement of sustainability goals make their construction worthwhile.

B. STRUCTURAL AND ACOUSTIC MODELS

The structural model was based on concrete slab checks necessary for the structural design of a one-way concrete slab system. This structural model utilized the American Concrete Institute (ACI) 318-19 structural concrete design code for the structural checks [21]. The structural methodology included the following steps: (1) determine the structural material properties and the factored loads on the concrete slab; (2) determine the ACI ductility requirements in the concrete slab; (3) conduct the structural analysis by calculating the flexural and shear capacities; and (4) check to ensure that the slab design satisfies the ACI design requirements. To conduct the structural analysis of the concrete slab, the slab was cut into longitudinal sections by the number of shaped ribs (shown in Figure 2). Therefore, the analysis was conducted on a rib of the slab, including both the top slab and the shaped rib. The single rib was cut into cross-sections to interpolate the necessary structural forces to meet the structural requirements. Due to the longitudinal curvature of the shaped rib, it was important to take many cuts across the rib from one end to the center of the rib. But since there is symmetry from rib end to end, only half of the cross sections were necessary to perform the structural evaluations. After obtaining the cross section, the applied structural forces were found for each slice and were evaluated to the ACI structural strength and design checks. The structural strength and design checks were applied as penalty functions in the optimization simulations. If each cross section satisfied the checks, then the slab was classified as a structurally qualified slab.

It is essential to identify the slab designs that are structurally sound per building design code. However, optimization requires a structural performance evaluation beyond the binary code checks. Thus, the shaped slabs' structural mass, as denoted as surface density, serves as one of the two objectives. While all simulations were conducted for a square one-way floor slab with a typical beam spacing of 6 m, the conversion to surface density allows for easier comparison outside of this fixed dimension. The surface density equates to the entire slab's mass, including both the concrete slab and the longitudinal steel reinforcement, divided by the slab's area. A design with lower surface density has less structural material which corresponds to less embodied carbon [22]. Structurally qualified slabs with shaped ribs are optimized for maximum surface density savings, but also account for acoustic performance.

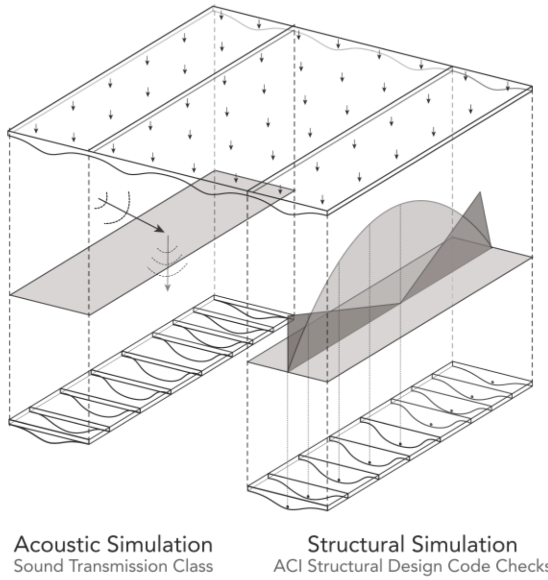

Figure 2. Acoustic and structural simulation.

In a similar manner, the shaped slab geometry was sectioned to evaluate the acoustic characteristic of transmission. To differentiate between shaped slab designs with similar mass but different geometry, an analytical model incorporating the transmission coefficient was performed. This included the slab's structural mass, damping, and stiffness. The structural mass was calculated based on the slab's geometric volume. The slab's damping was held constant for the acoustic analysis. The slab's stiffness was impacted by the top slab and the curved rib sections. The analytical transmission model was able to find the transmission loss of a structure by calculating a transmission coefficient, τ, for the structure as if it were an infinite panel as seen in the Eq. 2. The transmission coefficient is dependent on both the angle of incidence, φ, and the angular frequency, ω. The remaining variables to calculate the transmission coefficient include the density of air, ρ_0, the speed of sound of air, c_0, the damping coefficient of concrete, η, the flexural rigidity, D, wavenumber, k_0, and mass density, m, of the structural slab. It should be noted that the density of air, the speed of sound of air, and the damping coefficient of concrete were kept constant. The angle of incidence was also held constant at an angle of 45°.

$$\tau(\varphi,\omega) = \frac{(\frac{2\rho_0 c_0}{sin\varphi})^2}{(\frac{2\rho_0 c_0}{sin\varphi}+\eta(\frac{D}{\omega})(k_0 sin\varphi)^4)^2+(\omega m-(\frac{D}{\omega})(k_0 sin\varphi)^4)^2} \quad (2)$$

However, since the analytical transmission model finds transmission loss values for the slab, the transmission loss values are a function of frequency. To quantify the acoustic performance as a single integer, the acoustic metric of Sound Transmission Class (STC) was used. Despite the simplification of the acoustic model, STC is a good acoustic metric for optimization. This is due to how acoustic performance can be simplified to one number that attempts to quantify the overall performance, rather than the transmission loss for a single frequency [23]. The International Building Code and many local residential building codes require a minimum of STC-50 for structures within buildings [24]. So, to be classified as an acoustically qualified design in the model, the shaped concrete slab must have an STC-50 rating or higher. Fully qualified designs, which are the designs that are the desired solutions for building design, must be both structurally and acoustically qualified.

C. DESIGN SPACE EXPLORATION TECHNIQUES

To evaluate the fully qualified designs, three design space exploration techniques were used in sequence to investigate design trade-offs between structural and acoustic performance: Latin Hypercube Sampling (LHS), Multi-Objective Optimization (MOO), and Constrained Optimization (CO). The sequential order does not suggest dependence from one technique to the next as the techniques are independent of each other. For this and similar problems, it is anticipated that the order of the design space exploration techniques increases in resolution towards the best shaped slab designs with each method providing unique conclusions of the design space. The three design space exploration techniques were computed using the open-source plug-in Design Space Exploration [25].

Latin Hypercube Sampling of the design space provided broad insight on structural-acoustic trade-offs when initially exploring the design space. LHS did not select a completely random sample, but selected samples that had varying geometric differences to ensure that the full extent of the design space was sampled [16]. The selected designs were then evaluated for performance and mapped onto a bi-objective plot, which is a visualization of the objective space. The sampled objective space is insightful as it indicated trends in the design space that can be explored with further evaluation of the objectives. In addition, LHS showed the general trends within the design space that are not biased towards the best performing designs.

For Multi-Objective Optimization, the algorithm NSGA-II was used to explore the design space [17]. A population of 100 and generation size of 50 were specified so that the algorithm could create design mutations within the parametric model that had the best objective performance. A Pareto front approximation was obtained, as the later generation of the NSGA-II converged on some of the best designs yet determined. Penalty functions were applied to allow NSGA-II to evaluate the entire design space, considering designs that did not meet the structural strength design checks. The penalty functions were implemented as cubic functions added to the slab's surface density objective based on the structural check's percent error cubed (Eq. 3-5), applied only if the design failed. This enabled the algorithm to consider designs that barely failed while rejecting designs that failed significantly. While the algorithm does initially investigate a wide number of designs with a variety of geometric features, the algorithm attempts to converge to the non-dominated designs and therefore has a design space biased towards the best performing designs. In the penalty and structural check equations, φ represents the strength reduction factor, not the angle of incidence as in Eq. 2. The variables described in these equations include the factored flexural strength, M_u, the nominal flexural strength, M_n, the factored shear strength, V_u, the nominal shear strength, V_n, the minimum allowable area of longitudinal steel reinforcement, $A_{s,min}$, the provided area of longitudinal steel reinforcement, A_s, and the maximum allowable area of longitudinal steel reinforcement, $A_{s,max}$.

$$Shear\ Penalty = (|V_u - \varphi V_n|)^3 \tag{3}$$

$$Flexural\ Penalty = (|M_u - \varphi M_n|)^3 \tag{4}$$

$$Ductility\ Penalty = \left(\left|\begin{matrix} A_{s,min} - A_s \\ A_s - A_{s,max} \end{matrix}\right|\right)^3 \tag{5}$$

Constrained Optimization is another optimization method which identified the best performing designs, but the algorithm was based on the enactment of several constraints. A single objective is selected for optimization while constraining the other objectives and any other constraints using a gradient-free algorithm called COBYLA [20]. This work conducted CO simulations that minimized structural mass (Eq. 6) subject to a specific STC rating (Eq. 7), structural checks (Eq. 8-11), and geometric constraints (Eq. 12-14). An advantage of CO over MOO is that each constraint was evaluated individually instead of amalgamated as a single penalty function for each unique geometric permutation.

$$minimize\ f(x) = (structural\ mass) \tag{6}$$

$$\text{subject to } STC \geq [50,55,60,65] \tag{7}$$

$$M_u < \varphi M_n \tag{8}$$

$$V_u < \varphi V_n \tag{9}$$

$$A_{s,min} < A_s \tag{10}$$

$$A_s < A_{s,max} \tag{11}$$

$$Slab\ Thickness \geq \frac{Slab\ Length}{21} \tag{12}$$

$$Flange\ Width \geq Rib\ Spacing \tag{13}$$

$$Clear\ Cover \geq 1.5\ inches \quad (14)$$

As seen above, Eq. 8-14 describe the structural strength and design constraints. Eq. 8 and Eq. 9 constrain the design to sufficiently resist bending and shear forces. Eq. 10 and Eq. 11 constrain the steel reinforcement size utilized in the concrete slab design, corresponding to the slab's ductility. Lastly Eq. 12-14 describe the structural design constraints to ensure that the design satisfies structural building code.

An important practical consideration with these computational techniques is that they should be well suited for the timescale that the designer and engineer have. For the early design explorations in this research, many different optimization runs were conducted while adjusting the design space, determining the sensitivity of various parameters, and comparing the merits of optimization approaches. The approach of using rapid, iterative optimization runs stems from the main research questions, which include evaluating the nature of performance trade-offs in addition to identifying potentially high-performance designs.

While specific optimization settings are explained in the following section, details about the computational environment are provided here. The LHS simulations were conducted at a resolution of n = 5,000 on a desktop computer with an Intel® Core™ i7-7700 CPU @ 3.60GHz processor and 8.00 GB of RAM. In this environment, a single function evaluation took approximately 7 seconds, so the overall computation time for LHS was 9.37 hours. For the MOO results, NSGA-II was run with a population of 100 and a fixed generation of 50. This was intentionally chosen to approximate the computation time for sampling in order to compare the relative merits of each method. The MOO run was completed in 11.30 hours, a bit longer than sampling due to the algorithm's implementation. For the CO runs, convergence criteria such as STC rating and structural strength checks were established, rather than a fixed generation size. CO would then converge to the smallest structural mass obtainable while maintaining all constraints. As such, there was significant variability in the length of each run as the computational algorithm evaluated a couple hundred to several hundred designs. However, CO generally converged to the results in approximately 40 minutes.

4. RESULTS AND DISCUSSION

The following results visually demonstrate three design space exploration techniques. Figure 3 shows that each shaped slab design in the design space corresponds to a point in the bi-objective space. The designs are plotted for their performance of the two objectives: structural mass, as expressed by surface density, and Sound Transmission Class (STC). The following results are all plotted in the objective space, in which the STC axis has been inverted such that high performing designs trend towards the lower left quadrant, similar to classic optimization visualizations. In these plots, the non-dominated designs are often highlighted, which depending on the Design Space Exploration (DSE) technique, represents a low to high resolution Pareto front approximation. Some of the best shaped slab designs are specifically called out to identify geometric tendencies and structural-acoustic trade-offs.

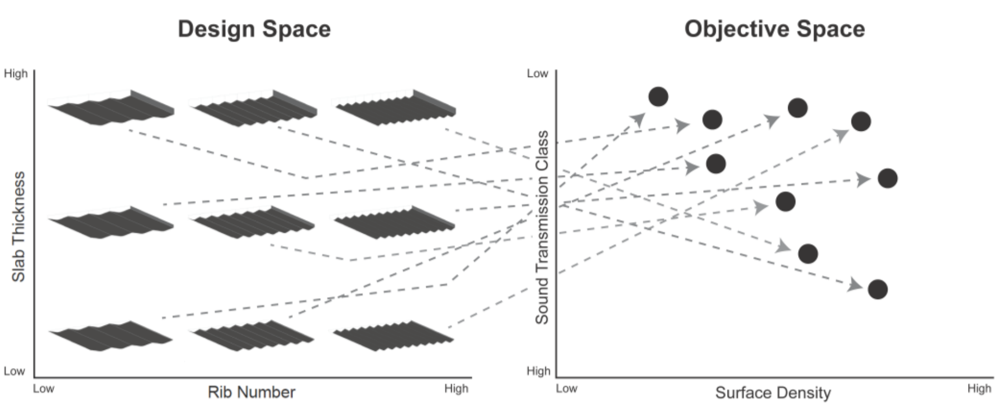

Figure 3. (Left) Nine shaped slabs are plotted on a 2D snapshot of the design space and (Right) objective space.

The design space was first explored using LHS at a resolution of 5,000 instances to evaluate the largest number of diverse designs across the full variable bounds. The sampled designs were mapped onto the objective space as shown in Figure 4 (left) using an analytical transmission model. For reference, conventional concrete slabs have similar surface density and STC relationships similar to the extent of this (left) objective space. Before the objective space was evaluated for the identification of the qualified designs, broad structural-acoustic trends were found. LHS showed that as the surface density increased, the potential for the slab's STC increased. The relationship is generally logarithmic as seen from STC-40 to STC-55, but then the relationship dramatically changes as considerably larger STC ratings become possible. To investigate this region, the objective space was classified by the one-third octave band frequency in which the coincidence dip occurs. The coincidence dip occurs when the wavelength of the air matches the structural wavelength of the slab. At this frequency, the slab acts as an efficient radiator of sound, hence lowering the designs' acoustic performance. Figure 4 (right) shows the breakdown of coincidence frequencies for the slab's that are structurally qualified: about 40% of the designs in the unqualified objective space were classified as structurally qualified designs. The coincidence dip was classified based on the bounds of the nearest one-third octave band.

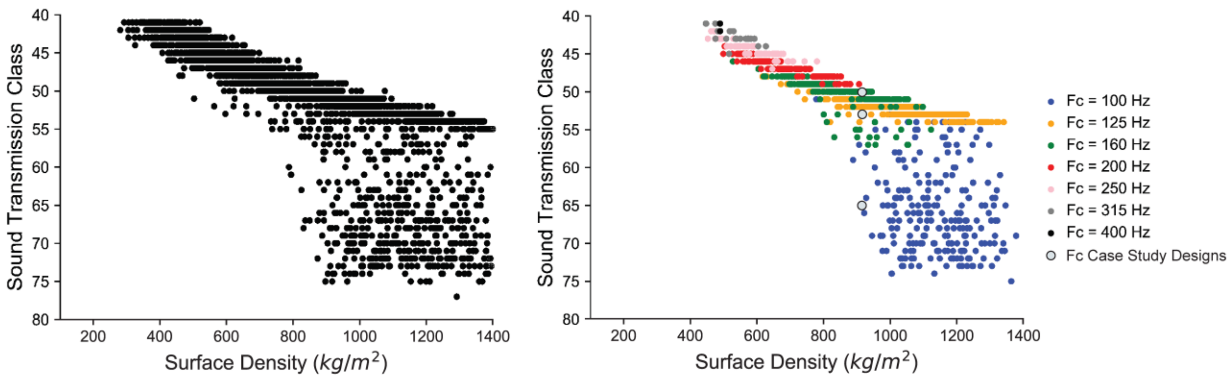

Figure 4. (Left) The objective space generated from LHS. (Right) The structurally qualified objective space classified by coincidence frequency.

The slabs had a range of coincidence frequencies, from the one-third octave bands of 100 Hz to 400 Hz. Yet the fully qualified designs only had coincidence frequencies from the one-third octave bands of 100 Hz to 160 Hz. In terms of the trend found from LHS, the region above STC-55 is dominated by slab designs that had a coincidence frequency in the 100 Hz one-third octave band. The coincidence frequency clustering also revealed that as the surface density increased, the coincidence frequency generally decreased, therefore potentially increasing the STC rating. To further investigate the trend, a case study (shown in Figure 5) was performed to evaluate three fully qualified designs that have coincidence frequencies within the 100 Hz, 125 Hz, and 160 Hz one-third octave bands.

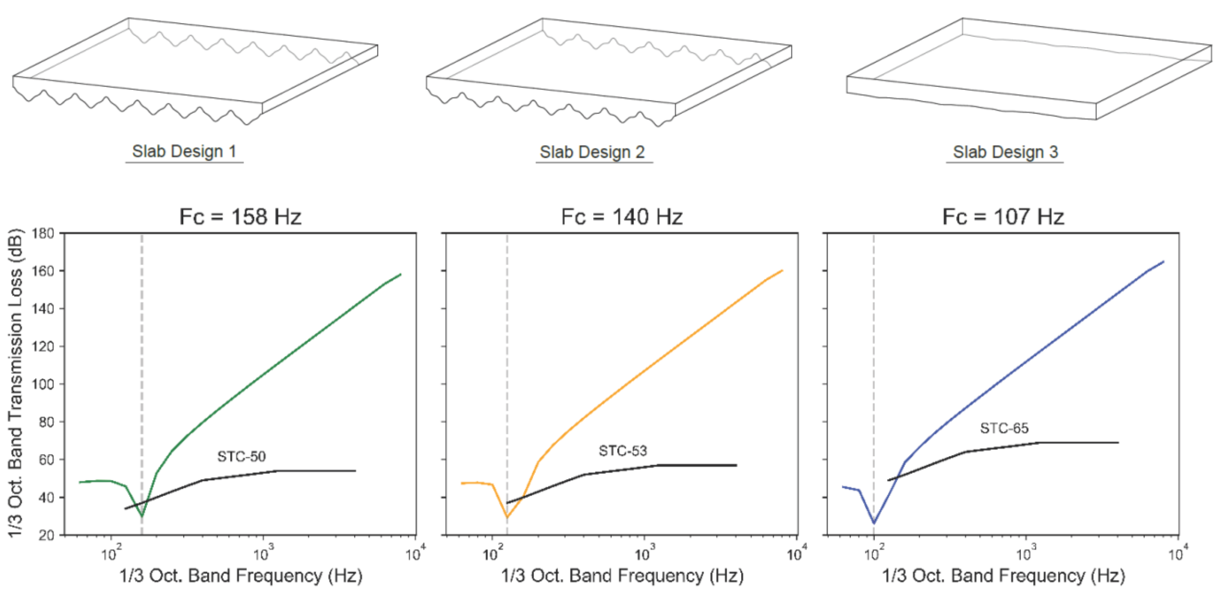

Figure 5. (Top) Coincidence frequency case study designs. (Bottom) The one-third octave center band TL versus frequency for the case study designs.

STC is only characterized with a frequency range of 125 Hz to 4,000 Hz. Since the coincidence dip is outside of this frequency region for the third case study design, the STC rating increased significantly as the metric did not account for the coincidence dip. The STC contour also showed why the designs with a coincidence frequency within the one-third octave bands of 160 Hz is mixed. Since the lowest number of the STC contour is at 125 Hz, the slab designs with shallow coincidence dips at 160 Hz may have higher STC ratings than slab designs with a coincidence frequency within the one-third octave band of 125 Hz.

Despite STC's limitation to meaningfully capture the coincidence frequency across all shaped concrete slab designs, the acoustic metric still has merit. STC is a measurement describing the amount of TL in the speech frequency range and is well integrated in the building industry. Although low frequency sounds may occur from other sound sources, the speech frequency is fully accounted for in STC. Though the coincidence dip may fall below this range, the slab designs with a coincidence dip lower than 125 Hz are still accurately quantified according to speech transmission. Therefore, the slab designs in the region characterized by having a coincidence frequency at 100 Hz are not excluded as acoustically qualified designs. The fully qualified objective space is shown in Figure 6 seen below.

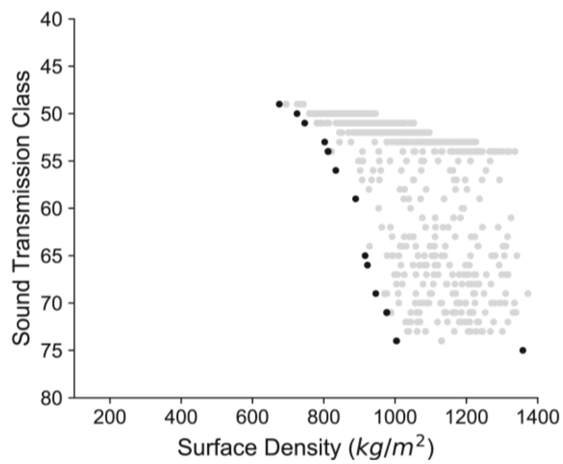

Figure 6. Estimation of the Pareto front found by LHS.

The fully qualified objective space found from LHS also suggested where the Pareto front occurs as indicated by the darkened points in Figure 6. The Pareto front is a collection of the non-dominated slab designs for which one objective cannot be improved without a decrease in performance for the other. This Pareto front is only a low-level estimation by LHS, as its evaluation was nearly randomized. Since the Pareto front was just approximated using LHS, a computational algorithm that converged on the best designs was needed. Therefore, Multi-Objective Optimization was used to converge to a higher resolution Pareto front.

Unlike LHS, MOO utilized a genetic, evolutionary algorithm (NSGA-II) to progressively approximate the set of non-dominated designs. MOO was conducted with two primary objectives while incorporating the structural strength and design checks as penalty functions. Penalty functions were applied for the structural checks to enable the algorithm to work through the entire design space, as the algorithm could manipulate a high-quality design that nearly passed. Figure 7 (left) displays the fully qualified objective space found by MOO.

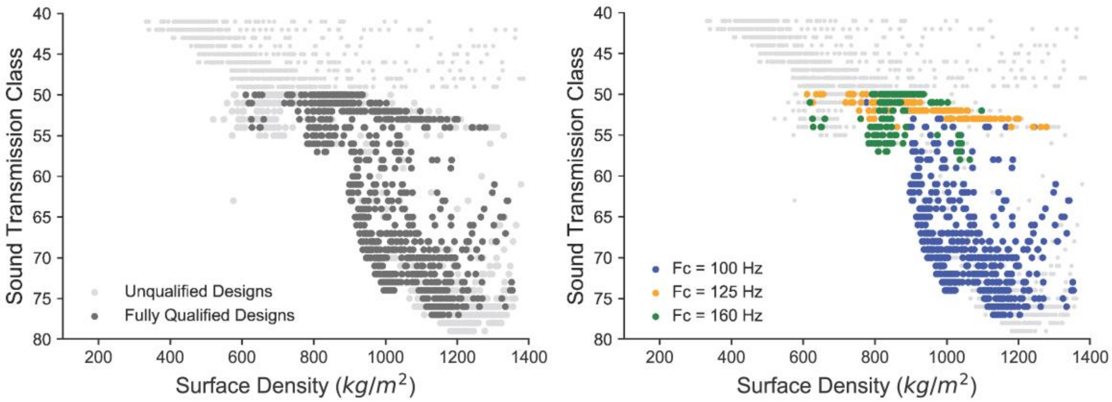

Figure 7. (Left) The objective space generated from MOO. (Right) The fully qualified objective space classified by coincidence frequency.

The same broad trend found by LHS is confirmed by MOO, that as the surface density increased, the potential for better acoustic performance increased. When assessing the slabs' coincidence frequencies found by MOO, the fully qualified designs have the same range of coincidence frequencies that were found by LHS. Additionally, the region of high STC rating is dominated by slab designs with a coincidence dip below 125 Hz, as indicated in Figure 7 (right). However, the trend that as the surface density increased the coincidence frequency decreased is harder to identify. This suggests that MOO, with a limited number of evaluations, may not be able to provide the clearest insight on trade-offs in the objective space when compared to LHS. MOO does not show the general design space trends as clearly as LHS because the design space becomes more biased towards better performing designs as the generation increases. Further research is needed for MOO for improved trade-off results. Yet despite these disadvantages, MOO does have a significant advantage to LHS, because engineers are generally looking for high-performance solutions and MOO finds them more efficiently and at higher concentration.

The algorithm utilized by MOO also pushed the objective space farther left, meaning that MOO found better performing designs than LHS. With the set population and generation sizes, the comparison of computation time showed that MOO took 20.6% longer than LHS. This is not an insignificant amount, but the difference of obtaining the best performing shaped slab designs suggests that MOO should be used. Furthermore, running more iterations could have improved the Pareto front found by MOO, but due to the increased computation time, an algorithm that could find the single best design at a known objective performance was considered advantageous. It was hypothesized that CO could outperform or match the best performing slab designs found by MOO since it converged on the best design given a constrained objective. As a consequence, the Pareto front must be evaluated at specific points and would take longer to estimate the full extent of the front.

Constrained optimization was conducted using the gradient-free algorithm COBYLA and was iterated four times at four different acoustic performance levels. The four acoustic performance levels quantified how well the structural slab prevented sound transmission as previously mentioned. The initial starting point for the CO simulations were the best performing designs previously found by MOO. CO then optimized the design by reducing the surface density while preserving the acoustic objective. The designs found by CO are compared to the best designs found from MOO as seen in Figure 8.

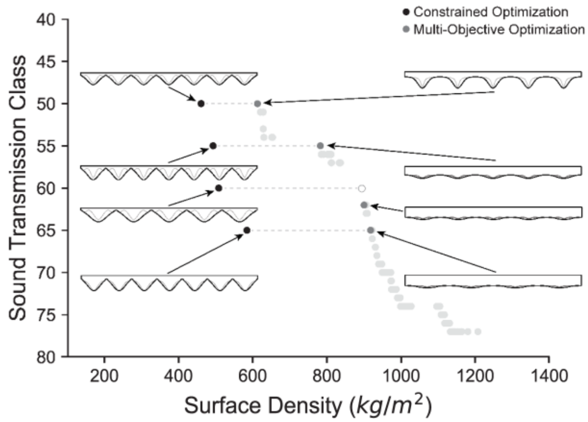

Figure 8. Comparison of best shaped slab designs found by CO and MOO.

Figure 8 revealed that the four simulations of CO significantly outperform the best shaped slab designs found by MOO. The geometric characteristics of the CO slabs appear very curved compared to the MOO slabs, especially at higher STC ratings. This indicates that constraining the acoustic objective has a significant impact on the result. Additionally, the large difference between CO and MOO can be explained with the constraint of longitudinal steel reinforcement in the design of a concrete slab. For this study on shaped concrete slabs, the parametric model suggested a steel reinforcement size for the slab design, therefore automating the selection when LHS and MOO are run. However, the steel reinforcement sizing was a constraint for the simulations and resulted in the better performing slab designs. This level of specificity in applying the reinforcement directly clearly provided a significant advantage in exploring the space.

Another advantage of CO is that it is likely to find a more structurally efficient design at a specific STC level than a MOO algorithm. However, a single constrained optimization run requires considerable computation to converge to only one shaped slab design (about 0.67 hours), and thus it is more difficult to identify a smooth, full Pareto front. The computation time to perform 20 CO simulations would be about 13.4 hours, which would be approaching 150% of the computation time of LHS. There is thus a trade-off between finding the best designs versus obtaining the general design space trends between the three design space exploration techniques. Therefore, general trends within the design space cannot be obtained when using constrained optimization.

When comparing the three design space exploration techniques, each of the techniques have both advantages and disadvantages. Figure 9 details the comparison between the three computational methods and confirms that there is not one single technique that can find both the best designs in the design space while fully exploring the extent of the design space as seen in Figure 10. As the resolution of finding the best shaped slab designs increased, the ability to find the trade-offs in the design space decreased and vice versa. As a result, this suggests that utilizing multiple design space exploration techniques, as done in this research would be beneficial in other case studies.

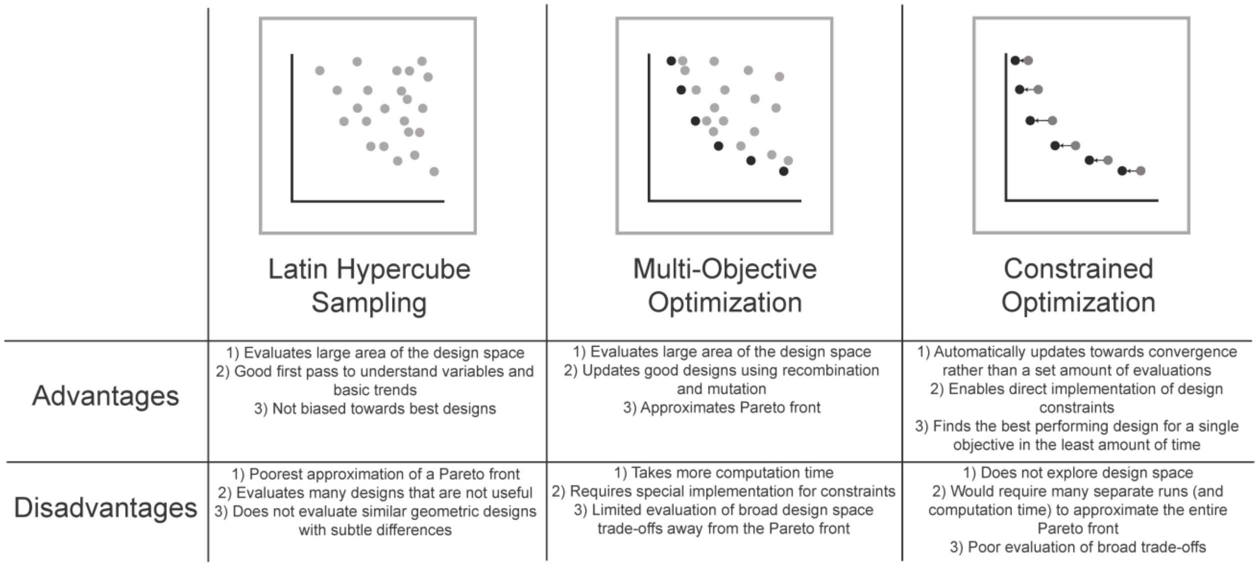

Figure 9. Comparison of the three design space exploration techniques.

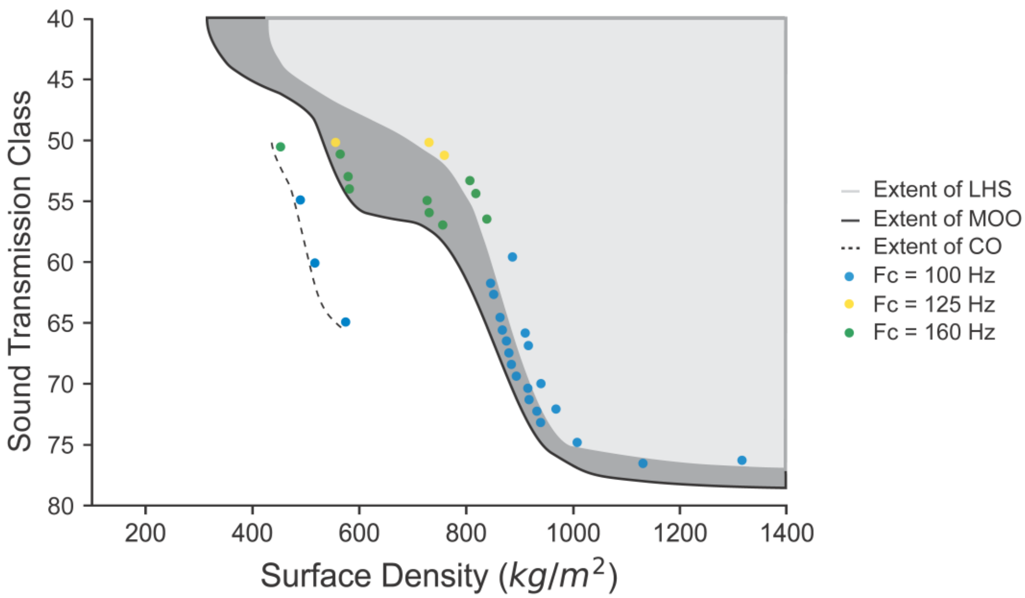

Figure 10. Comparison of the extent of the design space exploration techniques and classification of coincidence frequency.

Using a combination of design space exploration techniques was necessary for the thorough investigation of structural-acoustic shaped concrete slabs. As seen in Figure 10 above, the three techniques clearly show that better designs are obtained as the resolution to obtain the best designs increases. Yet, as the technique resolution increases, the design space does not show one of the important structural-acoustic trade-offs, which involves the coincidence frequency. LHS can show the relationship between the structural-acoustic performance and coincidence frequency while MOO only suggests it. Constrained optimization does not show this trend, however with more simulations, this trend could be found. It is important to note as well that the extents of the design space exploration techniques should be very close to each other, if given infinite computational time to iterate through the entire design space. However, since this study restricted the computational time to what would be a common computational time in design practice, there are differences in the techniques' extents.

5. CONCLUSION

This research investigated the utilization of three unique computational design space exploration techniques to evaluate the multi-objective performance of shaped concrete slabs. The optimization of shaped concrete slabs has shown that as the geometry becomes more complex, the structural and acoustic equations introduce linear and non-linear interactions. Broadly, as structural mass increases, the potential for higher sound transmission class (STC) increases. There is a positive logarithmic relationship between surface density and STC until between a rating of STC-55 and STC-60. Once this acoustic performance level is reached, STC greatly increases with little increase in surface density. This region of high increase in acoustic performance with little increase of surface density was generated due to the STC metric's exclusion of frequency evaluation below 125 Hz. These trends were originally found by sampling the design space and evaluating the objective performance for each slab using Latin Hypercube Sampling. Multi-Objective Optimization further investigated the objective space to find better performing shaped slab designs while also validating the broad structural-acoustic trade-offs found by LHS. Constrained Optimization was used to determine if single optimal designs found by MOO could be further improved.

This initial investigation of structural-acoustic trade-offs of shaped concrete slabs using multiple computational techniques reveals areas of further research. Since acoustic-based performance design is behind the performance design research in other building disciplines, more research should be conducted to include multi-objective studies with the other primary building consideration such as the architectural layout and geometric design. Beyond the application of other building applications, the utilization of other multi-objective algorithms and even machine learning could be informative and improve the incorporation of acoustics at the component level in the early stage of design. A study including more geometric features and layering of materials could provide further insights into the performance evaluation of shaped concrete slabs. The inclusion of an impact noise metric would provide further insight on how well the shaped slabs perform acoustically. Finally, a novel acoustic rating that combines both airborne and structural borne transmission should be considered in a multi-objective study.

ACKNOWLEDGMENTS

The authors would like to thank Mohamed Ismail of the MIT Digital Structures group for his assistance with the coded ACI structural design components.

REFERENCES

[1] E. Badino, L. Shtrepi, and A. Astolfi, "Acoustic performance-based design: a brief overview of the opportunities and limits in current practice," Acoustics. **2**(2), 246-278 (2020).

[2] C. Field, "Acoustic design in green buildings," ASHRAE Journal, (2008).

[3] S. N. Kamaruzzaman, A. Razali, A. Zawawi, and M. Riley, "Factors affecting indoor environmental quality and potential health risks of housing residents," in National Invention and Innovation Through Exhibition Competition Conference 2017, (2018).

[4] B. Rasmussen, "Sound insulation between dwellings - requirements in building regulations in Europe," Applied Acoustics. **71**(4), 373-385 (2010).

[5] N. Moeller, "Retrofitting Sound Masking: Improved speech privacy and noise control in occupied spaces," LogiSon Acoustic Network (2014).

[6] T. Méndez Echenagucia, N. B. Roozen, and P. Block, "Minimization of sound radiation in doubly curved shallow shells by means of structural stiffness," in Proceedings of the IASS Annual Symposium 2016, Spatial Structures in the 21st Century, 1-10 (2016).

[7] N. B. Roozen, Q. Leclère, D. Urbán, T. Méndez Echenagucia, P. Block, M. Rychtáriková, C. Glorieux, "Assessment of the airborne sound insulation from mobility vibration measurements; a hybrid experimental numerical approach," Journal of Sound and Vibration, **432**, 680-698 (2018).

[8] S. Marburg, M. R. Shepherd, S. A. Hambric, "Structural – Acoustic Optimization. Engineering vibroacoustic analysis: methods and applications (1st ed.)," John Wiley & Sons, 268-304 (2016).

[9] W. M. Johnson and K. A. Cunefare, "Structural acoustic optimization of a composite cylindrical shell using FEM/BEM," Journal of Vibration and Acoustics, Transactions of the ASME, **124**(3), 410-413 (2002).

[10] A. K. Nandy and C. S. Jog, "Optimization of vibrating structures to reduce radiated noise," Structural and Multidisciplinary Optimization. **45**(5), 717-728 (2012).

[11] M. R. Shepherd and A. S. Hambric "Structural-acoustic optimization of a pressurized ribbed panel," Proceedings of Meetings on Acoustics. **22**, 1-13 (2015).

[12] P. Wennhage, "Weight optimization of large scale sandwich structures with acoustic and mechanical constraints," Journal of Sandwich Structures and Materials **5**(3), 253-266 (2003).

[13] A. Berry and J. Nicolas, "Structural acoustics and vibration behavior of complex panels," Applied Acoustics **43**(3), 185-215 (1994).

[14] C. F. Ng and C. K. Hui, "Low frequency sound insulation using stiffness control with honeycomb panels," Applied Acoustics **69**(4), 293-301 (2008).

[15] E. Touloupaki and T. Theodosiou, "Optimization of building form to minimize energy consumption through parametric modeling," Procedia Environmental Sciences **38**, 509-514 (2017).

[16] M. Mckay, R. Beckham, and C. William, "A comparison of three methods for selecting values of input variables in the analysis of output from a computer code," Technometrics **21**, 239-245 (1979).

[17] K. Deb, A. Pratap, S. Agarwal, and T. Meyarivan, "A fast and elitist multi-objective genetic algorithm: NSGA-II," IEEE Transactions on Evolutionary Computation **6**(2), 182-197 (2002).

[18] T. Blanchet, J. Fournier, and T. Piketty, "Generalized Pareto curves: theory and applications," World Wealth & Income Database: The Source for Global Inequality Data (2017).

[19] C. A. McCormick and M. R. Shepherd, "Design optimization and performance comparison of three styles of one-dimensional acoustic black hole vibration absorbers," Journal of Sound and Vibration **470**, 1-12 (2020).

[20] A. Brownlee and J. Wright, "Constrained, mixed-integer and multi-objective optimization of building designs by NSGA-II with fitness approximations," Applied Soft Computing **33**, 114-126 (2015).

[21] ACI Committee and American Concrete Institute, "Building code requirements for structural concrete (ACI 318-19): An ACI Standard: commentary on building code requirements for structural concrete (ACI 318R-19) an ACI report," American Concrete Institute (2019).

[22] A. Zeitz, C. T. Griffin, and P. Dusicka, "Comparing the embodied carbon and energy of a mass timber structure system to typical steel and concrete alternatives for parking garages," Energy & Buildings **199**, 126-133 (2019).

[23] M. Long, "Architectural Acoustics (2nd ed.)," Elsevier Science & Technology (2014).

[24] International Code Council (ICC), "2018 International Building Code," International Code Council (2018).

[25] N. C. Brown, V. Jusiega, and C. T. Mueller, "Implementing data-driven parametric building design with a flexible toolbox," Automation in Construction, **118**, 1-16 (2020).